

A highly correlated topological bubble phase of composite fermions

Received: 7 June 2022

Accepted: 23 December 2022

Published online: 02 February 2023

 Check for updates

Vidhi Shingla^{1,4}, Haoyun Huang^{1,4}, Ashwani Kumar², Loren N. Pfeiffer³, Kenneth W. West³, Kirk W. Baldwin³ & Gábor A. Csáthy¹✉

Strong interactions and topology drive a wide variety of correlated ground states. Some of the most interesting of these ground states, such as fractional quantum Hall states and fractional Chern insulators, have fractionally charged quasiparticles. Correlations in these phases are captured by the binding of electrons and vortices into emergent particles called composite fermions. Composite fermion quasiparticles are randomly localized at high levels of disorder and may exhibit charge order when there is not too much disorder in the system. However, more complex correlations are predicted when composite fermion quasiparticles cluster into a bubble, and then these bubbles order on a lattice. Such a highly correlated ground state is termed the bubble phase of composite fermions. Here we report the observation of such a bubble phase of composite fermions, evidenced by the re-entrance of the fractional quantum Hall effect. We associate this re-entrance with a bubble phase with two composite fermion quasiparticles per bubble. Our results demonstrate the existence of a new class of strongly correlated topological phases driven by clustering and charge ordering of emergent quasiparticles.

Landau's symmetry breaking paradigm provides a framework to classify phases described by local order parameters. Topological phases do not fit into this classification and are described instead by topological invariants. Topological phases are characterized by the formation of edge states and of an insulating bulk, and, in the vast majority of cases, symmetry breaking does not play any role. Indeed, the bulk of most ordinary topological phases, such as the integer quantum Hall state forming in the two-dimensional electron gas¹, is an Anderson insulator. As the Landau level filling factor moves away from an integer value, bulk quasiparticles are generated, which are randomly localized. Local scanning probes provided evidence for such randomly localized bulk quasiparticles². A representation of integer quantum Hall states with a finite quasiparticle density is shown in Fig. 1a.

In addition to ordinary topological phases characterized solely by topological invariants, there is a larger class of phases for which both topological and Landau-type orders need to be invoked. Such phases exhibit topologically protected edge states, while quasiparticles in

their bulk break various spatial symmetries. An example of such a phase is the Wigner solid forming in the flanks of integer quantum Hall states³, which is related to the Wigner solid forming in the extreme quantum limit⁴. In the limit of no disorder, quasiparticles in the bulk of this phase are thought to order on a triangular lattice, while edge states maintain integer quantization of the Hall resistance. So far, conditions of low enough disorder for the formation of these types of Wigner solids were met in two-dimensional electron gases confined to gallium arsenide semiconductor (GaAs)^{3–9} and to graphene¹⁰. Even though microscopic observation of charge order is still lacking, measurements of the pinning mode³, nuclear magnetic resonance charge topography⁵, the phonon mode⁶ and localization^{7–10} provide evidence of charge ordering in the bulk.

The complexity of charge order is known to increase in higher Landau levels, where more intricate broken symmetry topological phases are possible. Electronic bubble phases share the triangular lattice structure of the Wigner solid, but acquire an internal degree

¹Department of Physics and Astronomy, Purdue University, West Lafayette, IN, USA. ²Department of Physics, Monmouth College, Monmouth, IL, USA.

³Department of Electrical Engineering, Princeton University, Princeton, NJ, USA. ⁴These authors contributed equally: Vidhi Shingla, Haoyun Huang.

✉e-mail: gcsathy@purdue.edu

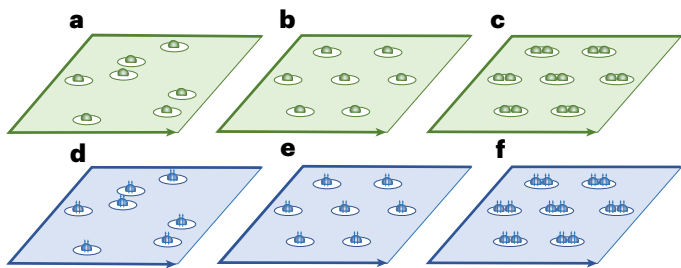


Fig. 1 | Representation of various topological phases of the electron gas with different bulk insulators. Spheres represent quasiparticles in the valence energy level, whereas coloured backgrounds represent the vacuum of the quasiparticles, that is, completely filled lower energy levels. In the top row, electron quasiparticle-based topological phases are shown. **a**, An ordinary topological phase with a bulk Anderson insulator. **b, c**, Topological phases with broken symmetry, described as electronic bubble phases with one (**b**) and two (**c**) electrons per bubble. The one-electron bubble phase is identical to the Wigner solid. In the bottom row, CFQP-based topological phases are shown. **d**, An ordinary topological phase with a bulk Anderson insulator of CFQPs. **e, f**, BPCFs with one (**e**) and two (**f**) CFQPs per bubble. The phase with one CFQP per bubble is identical to the WSCFs. The two vertical arrows attached to an electron reflect the vortex attachment procedure and account for Laughlin–Jastrow correlations. Arrows along the sample boundary represent edge states.

of freedom: each lattice node consists of clusters or bubbles of electron-like quasiparticles^{11,12}. A representation of this phase in the limit of no disorder with one and two quasiparticles per bubble is shown in Fig. 1b,c, respectively. Clearly, the one-quasiparticle electronic bubble phase is identical to the Wigner solid. They were predicted based on Hartree–Fock calculations performed in high Landau levels^{11,12} and were later found to proliferate in two-dimensional electron gases hosted in GaAs^{13–18}. More recently, they were also found in graphene¹⁹. Clustering of electrons into bubbles is energetically favourable because of the existence of nodes in the overlapping electronic wavefunctions^{11,12,18}.

Phases discussed so far support electron-like quasiparticles. Some of the most intriguing topological phases, such as fractional quantum Hall states (FQHs)^{20–22} and fractional Chern insulators^{23–25}, support fractionally charged quasiparticles that emerge from strong correlations. Such correlations were first captured by Laughlin's wave function²⁶ and later found a natural and intuitive description within the theory of composite fermions²⁷. Composite fermions are the emergent particles of this theory that form through binding of an even number of quantized vortices to electrons. Composite fermions experience an effective magnetic field that much reduced when compared to the externally applied field. In this description, the density of states of composite fermions consists of equally spaced energy levels called Λ -levels, and FQHs arise as composite fermions fill an integer number of Λ -levels²⁷. When a Λ -level is not fully filled, composite fermion quasiparticles (CFQPs) are generated²⁷. In the bulk of these FQHs, the CFQPs are randomly localized²⁸, as depicted in Fig. 1d.

When CFQPs interact in a low-disorder environment, the bulk may acquire charge order, and therefore broken symmetry topological phases with a highly correlated nature may form. Such interactions are especially important in flatband systems, such as the two-dimensional electron gas in a magnetic field. Indeed, due to their interactions, CFQPs were predicted to order into a Wigner solid of composite fermions (WSCFs)²⁹. A representation of the WSCFs is shown in Fig. 1e, and several numerical simulations have found evidence for their formation^{29–37}. However, because WSCFs and Wigner solids exhibit similar insulating behaviour, these phases cannot easily be distinguished by commonly employed experimental probes. Resonances detected in the microwave frequency domain in the vicinity of Landau level filling factor $v = 1/3$ were interpreted as being due to WSCFs³⁸.

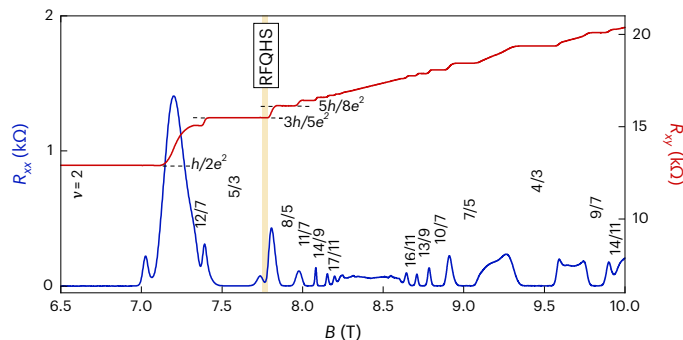


Fig. 2 | Magnetoresistance R_{xx} and Hall resistance R_{xy} over a broad range of magnetic fields B . Traces are obtained at the temperature $T = 12$ mK. Numerical labels indicate notable Landau level filling factors v at which one integer and several FQHs are shown. The structure of interest associated with the RFQHS develops near $B = 7.76$ T, located between Landau level filling factors $8/5 < v < 5/3$.

It is important to appreciate that the Wigner solid of electrons and WSCFs are not identical to each other. Indeed, the WSCFs has more intricate quantum mechanical correlations compared to those of the electron Wigner solid. These correlations are depicted in Fig. 1e as two vortices attached to each electron, and are embodied by a distinctive Laughlin–Jastrow term present in the many-body trial wave function of the WSCFs²⁹. The vortex attachment procedure can therefore be understood as a recipe for generating topological phases with strong, higher-order quantum mechanical correlations. Charge order with even more complex correlations was predicted when the vortex attachment procedure is applied to electronic bubble phases. The resulting phases are referred to as bubble phases of composite fermions (BPCFs)^{39,40}. A rendering of BPCFs with one and two CFQPs per bubble is shown in Fig. 1e,f, respectively.

Re-entrance of the $v = 5/3$ FQHS

We focus on magnetotransport in the fractional quantum Hall regime in the lowest Landau level, in the region centred on $v = 3/2$. Measurements are performed on a sample of density $n = 3.06 \times 10^{11} \text{ cm}^{-2}$ and mobility $\mu = 32 \times 10^6 \text{ cm}^2 \text{ V}^{-1} \text{ s}^{-1}$. Numerous FQHs of this region form at filling factors of the form $v = 2 - i/(2i + 1) = (3i + 2)/(2i + 1)$, where i is an integer⁴¹. The FQHs at $v = 5/3, 8/5, 11/7, 14/9, 17/11, 20/13$ seen in Fig. 2 belong to this sequence, with $i = 1, 2, 3, 4, 5, 6$. These FQHs are particle–hole symmetric counterparts of the ones forming at $v = i/(2i + 1)$ in the presence of the spin degrees of freedom. FQHs are identified by their vanishing longitudinal resistance $R_{xx} = 0$ and a Hall resistance quantized to the value $R_{xy} = (2i + 1)h/(3i + 2)e^2$. Here h is Planck's constant and e the elementary charge. According to composite fermion theory, this sequence of FQHs forms when spinful two-flux composite fermions fill an integer number of $i = 1, 2, 3, 4, 5, 6$ of Λ -levels^{27,41}. When the lowest Λ -level is completely filled, $i = 1$ and the ground state of the system is the $v = 5/3$ FQHS. Similarly, when two Λ -levels are completely filled, $i = 2$ and one obtains the FQHS at $v = 8/5$. Another series of FQHs forms at $v = 2 - i/(2i - 1)$ where $i = 2, 3, 4, 5, 6, 7$. Yet more FQHs seen in Fig. 2, such as the ones at $v = 9/7, 14/11$ and $12/7$, do not belong to these series. The local minimum in R_{xx} near the magnetic field $B = 7.06$ T does not signal an FQHS; instead, it was recently associated with the Wigner solid⁹.

Transport near $B = 7.76$ T exhibits a particularly interesting feature that breaks the typical pattern between two neighbouring FQHs. Indeed, neighbouring FQHs in the lowest Landau level are typically separated by a single peak in R_{xx} ²⁰. This is the case for data shown in Fig. 2 for the transition between the $v = 8/5$ and the $v = 11/7$ FQHs, the $v = 11/7$ and the $v = 14/9$ FQHs, and for numerous other neighbouring FQHs. However, transport in the transition region between the $v = 5/3$ and the $v = 8/5$ FQHs near $B = 7.76$ T is more complex: there are two R_{xx}

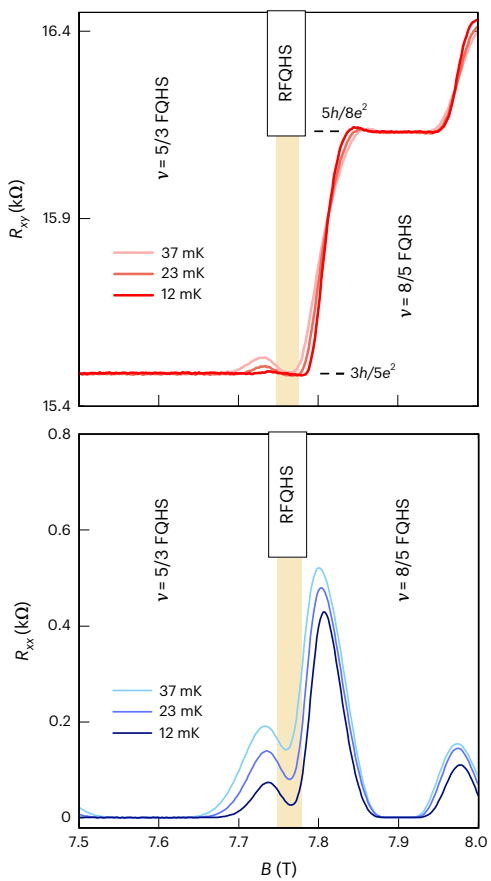


Fig. 3 | Magnetoresistance R_{xx} and Hall resistance R_{xy} at selected values of the temperature. The RFQHS and the nearby $v = 5/3$ FQHS are separated by a conspicuous signature in magnetotransport seen near $B = 7.73$ T, both in the longitudinal and Hall resistance: a local maximum in R_{xx} and a deviation from quantization in R_{xy} . Labels are temperatures measured in units of mK.

peaks that are separated by a vanishingly small R_{xx} . Furthermore, as seen in Fig. 2, the Hall resistance R_{xy} at $B = 7.76$ T at the lowest temperature is quantized to $3h/5e^2$. These details may be further examined in Fig. 3. Altogether, we report four instances of similar complex transport; three of these are shown in Extended Data Fig. 1 found in Supplementary Information. Extended Data Figure 1 demonstrates reproducibility after thermal cycling and the observation of similar behaviour in a second sample. In Supplementary Information we also discuss anomalies at this filling factor region reported in earlier work.

Complex transport behaviour between two consecutive FQHSs can be due to either a spin transition or an unusual ground state. However, the transport behaviour observed near $B = 7.76$ T is inconsistent with a spin transition for three reasons. First, a quantized Hall resistance we observe at $B = 7.76$ T is not expected near a spin transition^{41,42}. Second, the pattern of the longitudinal resistance measured near $B = 7.76$ T is different from that at a spin transition^{41,42}. Third, a spin transition is not expected in the $v = 5/3$ state⁴¹, but it is known to occur in the $v = 8/5$ state^{42,43}. However, this transition is strongly dependent on the width of the confining quantum well⁴². The density $3.06 \times 10^{11} \text{ cm}^{-2}$ of our 30 nm wide quantum well samples greatly exceeds the critical density at this width⁴², hence the $v = 8/5$ state in our sample forms deep inside the fully spin-polarized regime, far away from a spin transition. By ruling out a spin transition near $B = 7.76$ T, we ascertain that at this field there is a different ground state forming.

For insight on the unusual transport pattern near $B = 7.76$ T, we recall the transport phenomenology of the re-entrant integer quantum Hall states. These states are satellite formations near integer quantum

Hall states associated with electronic bubble phases^{13–19}. Both integer quantum Hall states and the re-entrant states are characterized by a vanishing R_{xx} and a quantized R_{xy} , but are separated from each other by a deviation from quantization. Transport behaviour near $B = 7.76$ T is similar: both the $v = 5/3$ state and the region near $B = 7.76$ T are characterized by a vanishing R_{xx} and a quantized R_{xy} , and they are separated by a deviation from quantization developing near $B = 7.73$ T. However, in contrast to the re-entrant integer states, the Hall resistance near $B = 7.76$ T is not quantized to an integer but rather to a fractional value $R_{xy} = 3h/5e^2$. Henceforth we will refer to the unusual transport developing near $B = 7.76$ T as the re-entrant fractional quantum Hall state (RFQHS), and we associate it with a new ground state of the system. From data shown in Fig. 4 we infer that transport signatures for the RFQHS survive in our sample to temperatures as high as 60 mK.

Candidate ground states for the RFQHS

To understand the nature of the RFQHS, we invoke composite fermion theory²⁷. As already discussed, at $v = 5/3$ there is an FQHS. At this filling factor the two-flux composite fermions completely fill the lowest Λ -level. An increasing B field in this region of filling factors results in a decrease of the effective magnetic field, which in turn leads to a decrease in the degeneracy of this Λ -level. An increasing B field past its value at $v = 5/3$ therefore generates CFQPs that reside in the second Λ -level. At relatively low densities, these CFQPs of the second Λ -level are Anderson-localized by the disorder present, contributing thus to the plateau of the $v = 5/3$ state.

Near $B = 7.73$ T, R_{xx} deviates from zero and R_{xy} deviates from quantization. Such transport signatures are associated with delocalized CFQPs in the bulk. However, at an even larger magnetic field $B = 7.76$ T, there is a return to a nearly vanishing R_{xx} , a quantized R_{xy} and thus to localization. However, localization near $B = 7.76$ T is inconsistent with an Anderson type of localization. Instead, the observed re-entrant behaviour constitutes evidence for a correlated CFQP insulator in which localization is generated by pinning of a charge-ordered phase. A quantized $R_{xy} = 3h/5e^2$ of both the correlated CFQP insulator forming at $B = 7.76$ T and the $v = 5/3$ state suggests the same CFQPs are involved in the formation of both ground states. We thus identify the RFQHS with a correlated CFQP insulator in which the CFQPs order into a topological phase with a broken symmetry. According to existing theory, candidate ground states for this correlated CFQP insulator can be described as BPCFs, specifically the ones with one CFQP and two CFQPs per bubble^{39,40}. There is therefore a close analogy between re-entrant integer quantum Hall states, interpreted as electronic bubble phases^{13–19}, and the RFQHS, interpreted as BPCFs. In Extended Data Fig. 2 of the Supplementary Information, we show that the lack of resistance anisotropy at $B = 7.76$ T is inconsistent with a stripe phase of CFQP interpretation of the RFQHS.

We now calculate the Λ -level filling factor v^* at which the RFQHS forms. We first find its electronic filling factor from the electron density n and the magnetic field B of formation $v = hn/eB = 1.628$. Then, v^* can be obtained from the $v = 2 - v^*/(2v^* + 1)$ relation⁴¹. The calculated $v^* = 1.45$ value means that at the formation of the RFQHS, there is one Λ -level completely filled and another only partially filled. In this partially filled second Λ -level, only a fraction $v_p^* = 0.45$ of the available states are filled. The quantity $v_p^* = 0.45$ represents the partial filling factor of the second Λ -level.

At $v^* = 1.45$, Hartree–Fock calculations predict that the BPCFs with one CFQP per bubble and those with two CFQPs per bubble are close in energy^{39,40}. A sketch of the former is shown in Fig. 1e, whereas the latter is depicted in Fig. 1f. However, for correlated states of high complexity, such as BPCFs, energy calculations are increasingly difficult, and drawing a conclusion on the nature of competing ground states close in energy is not straightforward. To further our understanding, we notice that the RFQHS forms at an unusually large Λ -level filling factor. Indeed, the partial Λ -level filling factor of the RFQHS is about a

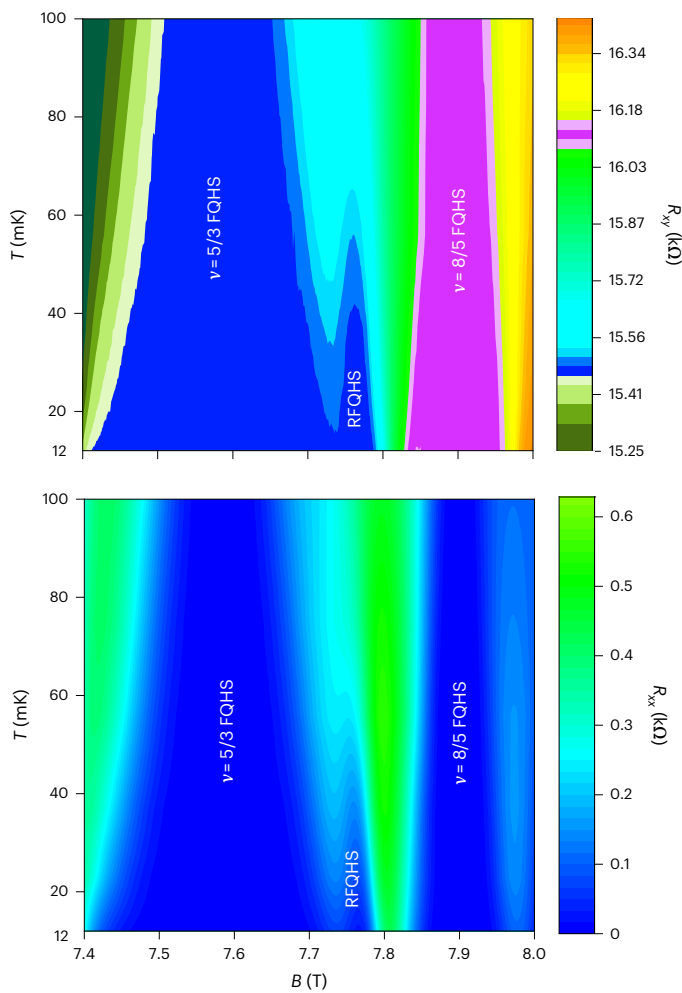


Fig. 4 | Magnetic field and temperature dependence of the magnetoresistance R_{xx} and Hall resistance R_{xy} for filling factors that include the $v = 5/3$ to $v = 8/5$ range. The bottom panel shows R_{xx} , whereas the top panel shows R_{xy} . The RFQHS is observed centred to $B = 7.76$ T at temperatures as high as 60 mK.

factor of 4 larger than that of the WSCFs reported in ref. ³⁸. A larger filling factor translates into a larger CFQP density, which is conducive to a more substantial overlap of the CFQP wavefunctions and thus may lead to correlations that otherwise are not possible. The essence of Hartree–Fock theories is that this wave function overlap affords new ways of minimizing the energy, through the formation of clusters of CFQPs, such as two-CFQP bubbles ^{39,40}. We think that the unusually large partial filling factor of the RFQHS favours an interpretation of BPCFs with two CFQPs per bubble.

The interpretation of the RFQHS as a BPCF with two CFQPs per bubble is further strengthened by a close analogy between electronic bubble phases and BPCFs. In high Landau levels, there are many electronic bubble phases ¹⁸, but they are not centred to a partial filling factor larger than 0.3. The only known electronic bubble phases at a large 0.44 partial filling factor form in the second Landau level ^{16,44}. According to Hartree–Fock calculations, these electronic bubble phases have two electrons per bubble ⁴⁵. An example of such a phase centred to a large partial filling factor is the one labelled as $R2b$ in ref. ⁴⁴. We notice that there is a close relationship between $R2b$ and the RFQHS. First, both of these bubble phases share their orbital quantum number of the relevant constituents. Indeed, $R2b$ forms in the second Landau level for electrons ^{16,44}, and the RFQHS forms in the second Λ -level for composite fermions. Furthermore, the partial filling factors of the topmost energy

level for both phases are unusually large and very close to each other: $v_p = 0.44$ for $R2b$ ⁴⁴ and $v_p^* = 0.45$ for the RFQHS. The close analogy between the two phases strengthens the interpretation of the RFQHS as a BPCF with two CFQPs per bubble.

Ground states at filling factors related by particle–hole symmetry are typically of a similar nature. It is thus worth examining the $1/3 < v < 2/5$ filling factor range, which is related to the $8/5 < v < 5/3$ range we studied by the $v \leftrightarrow 2 - v$ symmetry. Ground states in the $1/3 < v < 2/5$ range are FQHSs^{46,47}, such as the ones at $v = 4/11$ and $v = 3/8$. At the conjugate filling factors $v = 2 - 4/11 = 18/11$ and $v = 2 - 3/8 = 13/8$ our data do not exhibit FQHSs, since the Hall resistance measured at these filling factors does not exhibit plateaus consistent with FQHSs. Instead, we observe the BPCF at a filling factor that falls between 13/8 and 18/11. This difference in the type of ground states at symmetry-related filling factors is highly unusual and it remains to be studied both theoretically and experimentally. We surmise that either a symmetry breaking term in the Hamiltonian or differences in quasiparticle interactions are possible explanations. Interactions are tuned by sample parameters, such as the finite width of the quantum well and Landau level mixing, and even small changes in these parameters can stabilize fundamentally different types of ground states. The transition from the paired FQHS to the stripe phase as driven by the width and Landau level mixing parameter constitutes such an example⁴⁸.

We note that theories allow for WSCFs at CFQP densities lower than that of the BPCFs with two CFQPs per bubble. This phase would be signalled by full quantization, so it may already be present in our data; for example, near $B = 7.65$ T in Fig. 3. However, we found no transport signature that separates such a WSCF from an Anderson insulator forming in the centre of the $v = 5/3$ plateau, thus whether or not the WSCF forms near $v = 5/3$ remains an open question. A related problem in the integer quantum Hall regime is discussed in ref. ⁸.

It has long been recognized that the success of the composite fermion theory in describing FQHSs hinges on the nearly independent nature of the CFQPs. Indeed, interactions between CFQPs are greatly reduced as a result of the Chern–Simmons gauge forces associated with vortex attachment countering the strong Coulomb repulsion of electrons. However, because of the discreetness of the vortex attachment process, gauge forces do not always fully compensate the Coulomb repulsion. In such instances, the residual interaction between composite fermions may stabilize unusual ground states, such as the BPCF.

Online content

Any methods, additional references, Nature Portfolio reporting summaries, source data, extended data, supplementary information, acknowledgements, peer review information; details of author contributions and competing interests; and statements of data and code availability are available at <https://doi.org/10.1038/s41567-023-01939-2>.

References

1. Klitzing, K. V., Dorda, G. & Pepper, M. New method for high-accuracy determination of the fine-structure constant based on quantized Hall resistance. *Phys. Rev. Lett.* **45**, 494–497 (1980).
2. Zhitenev, N. B. et al. Imaging of localized electronic states in the quantum Hall regime. *Nature* **404**, 473–476 (2000).
3. Chen, Y. et al. Microwave resonance of the 2D Wigner crystal around integer Landau fillings. *Phys. Rev. Lett.* **91**, 016801 (2003).
4. Shayegan, M. Wigner crystals in flat band 2D electron systems. *Nat. Rev. Phys.* **4**, 212–213 (2022).
5. Tiemann, L., Rhone, T. D., Shibata, N. & Muraki, K. NMR profiling of quantum electron solids in high magnetic fields. *Nat. Phys.* **10**, 648–652 (2014).
6. Jang, J., Hunt, B. M., Pfeiffer, L. N., West, K. W. & Ashoori, R. C. Sharp tunnelling resonance from the vibrations of an electronic Wigner crystal. *Nat. Phys.* **13**, 340–344 (2017).

7. Liu, Y. et al. Observation of reentrant integer quantum Hall states in the lowest Landau level. *Phys. Rev. Lett.* **109**, 036801 (2012).
8. Myers, S. A., Huang, H., Pfeiffer, L. N., West, K. W. & Csáthy, G. A. Magnetotransport patterns of collective localization near $v=1$ in a high-mobility two-dimensional electron gas. *Phys. Rev. B* **104**, 045311 (2021).
9. Shingla, V., Myers, S. A., Pfeiffer, L. N., Baldwin, K. W. & Csáthy, G. A. Particle-hole symmetry and the reentrant integer quantum Hall Wigner solid. *Commun. Phys.* **4**, 204 (2021).
10. Zhou, H., Polshyn, H., Taniguchi, T., Watanabe, K. & Young, A. F. Solids of quantum Hall skyrmions in graphene. *Nat. Phys.* **16**, 154–158 (2020).
11. Koulakov, A. A., Fogler, M. M. & Shklovskii, B. I. Charge density wave in two-dimensional electron liquid in weak magnetic field. *Phys. Rev. Lett.* **76**, 499–502 (1996).
12. Moessner, R. & Chalker, J. T. Exact results for interacting electrons in high Landau levels. *Phys. Rev. B* **54**, 5006–5015 (1996).
13. Lilly, M. P., Cooper, K. B., Eisenstein, J. P., Pfeiffer, L. N. & West, K. W. Evidence for an anisotropic state of two-dimensional electrons in high Landau levels. *Phys. Rev. Lett.* **82**, 394–397 (1999).
14. Du, R. R. et al. Strongly anisotropic transport in higher two-dimensional Landau levels. *Solid State Commun.* **109**, 389–394 (1999).
15. Cooper, K. B., Lilly, M. P., Eisenstein, J. P., Pfeiffer, L. N. & West, K. W. Insulating phases of two-dimensional electrons in high Landau levels: observation of sharp thresholds to conduction. *Phys. Rev. B* **60**, R11285 (1999).
16. Eisenstein, J. P., Cooper, K. B., Pfeiffer, L. N. & West, K. W. Insulating and fractional quantum Hall states in the first excited Landau level. *Phys. Rev. Lett.* **88**, 076801 (2002).
17. Fu, X. et al. Two-and three-electron bubbles in $\text{Al}_x\text{Ga}_{1-x}\text{As}/\text{Al}_{0.24}\text{Ga}_{0.76}\text{As}$ quantum wells. *Phys. Rev. B* **99**, 161402 (2019).
18. Ro, D. et al. Electron bubbles and the structure of the orbital wave function. *Phys. Rev. B* **99**, 201111 (2019).
19. Chen, S. et al. Competing fractional quantum Hall and electron solid phases in graphene. *Phys. Rev. Lett.* **122**, 026802 (2019).
20. Stormer, H. L., Tsui, D. C. & Gossard, A. C. The fractional quantum Hall effect. *Rev. Mod. Phys.* **71**, S298–S305 (1999).
21. Du, X., Skachko, I., Duerr, F., Lucan, A. & Andrei, E. Y. Fractional quantum Hall effect and insulating phase of Dirac electrons in graphene. *Nature* **462**, 192–195 (2009).
22. Bolotin, K. I., Ghahari, F., Shulman, M. D., Stormer, H. L. & Kim, P. Observation of the fractional quantum Hall effect in graphene. *Nature* **462**, 196–199 (2009).
23. Spanton, E. M. et al. Observation of fractional Chern insulators in a van der Waals heterostructure. *Science* **360**, 62–66 (2018).
24. Xie, Y. et al. Fractional Chern insulators in magic-angle twisted bilayer graphene. *Nature* **600**, 439–443 (2021).
25. Pierce, A. T. et al. Unconventional sequence of correlated Chern insulators in magic-angle twisted bilayer graphene. *Nat. Phys.* **17**, 1210–1215 (2021).
26. Laughlin, R. B. Anomalous quantum Hall effect: an incompressible quantum fluid with fractionally charged excitations. *Phys. Rev. Lett.* **50**, 1395–1398 (1983).
27. Jain, J. K. Composite-fermion approach for the fractional quantum Hall effect. *Phys. Rev. Lett.* **63**, 199–202 (1989).
28. Martin, J. et al. Localization of fractionally charged quasi-particles. *Science* **305**, 980–983 (2004).
29. Yi, H. & Fertig, H. A. Laughlin-Jastrow-correlated Wigner crystal in a strong magnetic field. *Phys. Rev. B* **58**, 4019–4027 (1998).
30. Narevich, R., Murthy, G. & Fertig, H. A. Hamiltonian theory of the composite-fermion Wigner crystal. *Phys. Rev. B* **64**, 245326 (2001).
31. Chang, C. C., Jeon, G. S. & Jain, J. K. Microscopic verification of topological electron-vortex binding in the lowest Landau-level crystal state. *Phys. Rev. Lett.* **94**, 016809 (2005).
32. He, W. J. et al. Phase boundary between the fractional quantum Hall liquid and the Wigner crystal at low filling factors and low temperatures: a path integral Monte Carlo study. *Phys. Rev. B* **72**, 195306 (2005).
33. Chang, C. C., Töke, C., Jeon, G. S. & Jain, J. K. Competition between composite-fermion-crystal and liquid orders at $v=1/5$. *Phys. Rev. B* **73**, 155323 (2006).
34. Archer, A. C., Park, K. & Jain, J. K. Competing crystal phases in the lowest Landau level. *Phys. Rev. Lett.* **111**, 146804 (2013).
35. Zhao, J., Zhang, Y. & Jain, J. K. Crystallization in the fractional quantum Hall regime induced by Landau-level mixing. *Phys. Rev. Lett.* **121**, 116802 (2018).
36. Zuo, Z. W. et al. Interplay between fractional quantum Hall liquid and crystal phases at low filling. *Phys. Rev. B* **102**, 075307 (2020).
37. Archer, A. C. & Jain, J. K. Static and dynamic properties of type-II composite fermion Wigner crystals. *Phys. Rev. B* **84**, 115139 (2011).
38. Zhu, H. et al. Observation of a pinning mode in a Wigner solid with $v=1/3$ fractional quantum Hall excitations. *Phys. Rev. Lett.* **105**, 126803 (2010).
39. Lee, S. Y., Scarola, V. W. & Jain, J. K. Structures for interacting composite fermions: stripes, bubbles, and fractional quantum Hall effect. *Phys. Rev. B* **66**, 085336 (2002).
40. Goerbig, M. O., Lederer, P. & Smith, C. M. Possible reentrance of the fractional quantum hall effect in the lowest Landau level. *Phys. Rev. Lett.* **93**, 216802 (2004).
41. Du, R. R. et al. Fractional quantum Hall effect around $v=3/2$: composite fermions with a spin. *Phys. Rev. Lett.* **75**, 3926–3929 (1995).
42. Liu, Y. et al. Spin polarization of composite fermions and particle-hole symmetry breaking. *Phys. Rev. B* **90**, 085301 (2014).
43. Eisenstein, J. P., Stormer, H. L., Pfeiffer, L. N. & West, K. W. Evidence for a phase transition in the fractional quantum Hall effect. *Phys. Rev. Lett.* **62**, 1540–1543 (1989).
44. Deng, N. et al. Collective nature of the reentrant integer quantum Hall states in the second Landau level. *Phys. Rev. Lett.* **108**, 086803 (2012).
45. Goerbig, M. O., Lederer, P. & Smith, C. M. Competition between quantum-liquid and electron-solid phases in intermediate Landau levels. *Phys. Rev. B* **69**, 115327 (2004).
46. Pan, W. et al. Fractional quantum Hall effect of composite fermions. *Phys. Rev. Lett.* **90**, 016801 (2003).
47. Samkharadze, N., Arnold, I., Pfeiffer, L. N., West, K. W. & Csáthy, G. A. Observation of incompressibility at $v=4/11$ and $v=5/13$. *Phys. Rev. B* **91**, 081109(R) (2015).
48. Schreiber, K. A. & Csáthy, G. A. Competition of pairing and nematicity in the two-dimensional electron gas. *Annu. Rev. Condens. Matter Phys.* **11**, 17–35 (2020).

Publisher's note Springer Nature remains neutral with regard to jurisdictional claims in published maps and institutional affiliations.

Springer Nature or its licensor (e.g. a society or other partner) holds exclusive rights to this article under a publishing agreement with the author(s) or other rightsholder(s); author self-archiving of the accepted manuscript version of this article is solely governed by the terms of such publishing agreement and applicable law.

© The Author(s), under exclusive licence to Springer Nature Limited 2023

Methods

Data presented in the main text are generated from a sample we will refer to as Sample 1. Sample 1 is a two-dimensional electron gas confined to a 30 nm GaAs quantum well that is part of a GaAs/aluminum gallium arsenide (AlGaAs) heterostructure. Doping is done in a superlattice. The density of this sample is $n = 3.06 \times 10^{11} \text{ cm}^{-2}$ and the low-temperature mobility is $\mu = 32 \times 10^6 \text{ cm}^2 \text{ V}^{-1} \text{ s}^{-1}$.

Magnetotransport measurements were performed in a van der Pauw sample geometry using standard lock-in technique. The excitation current used was 3 nA. Our sample was mounted in vacuum on the copper tail of our dilution refrigerator, reaching the lowest estimated temperature of $T = 12 \text{ mK}$.

Sample states were prepared by illumination with a red light emitting diode located close to the sample and facing it. The illumination was performed near a sample temperature of 10 K, by passing a 4 mA current through the diode. Such an illumination slightly increases the sample density, and we believe it alleviates density inhomogeneities that may be present.

Data availability

Data are available upon request. Source data are provided with this paper.

Acknowledgements

We acknowledge useful discussions with J. Jain and V. Scarola. Measurements at Purdue were supported by the NSF DMR Grant No. 1904497. The sample growth effort of L.N.P., K.W.W. and K.W.B. of Princeton University was supported by the Gordon and Betty

Moore Foundation Grant No. GBMF 4420 and the National Science Foundation MRSEC Grant No. DMR-1420541.

Author contributions

V.S. and A.K. performed low-temperature transport measurements. L.N.P., K.W.W. and K.W.B. produced molecular beam epitaxy-grown GaAs/AlGaAs samples and characterized them. V.S., H.H. and G.A.C. analysed the data and wrote the paper.

Competing interests

The authors declare no competing interests.

Additional information

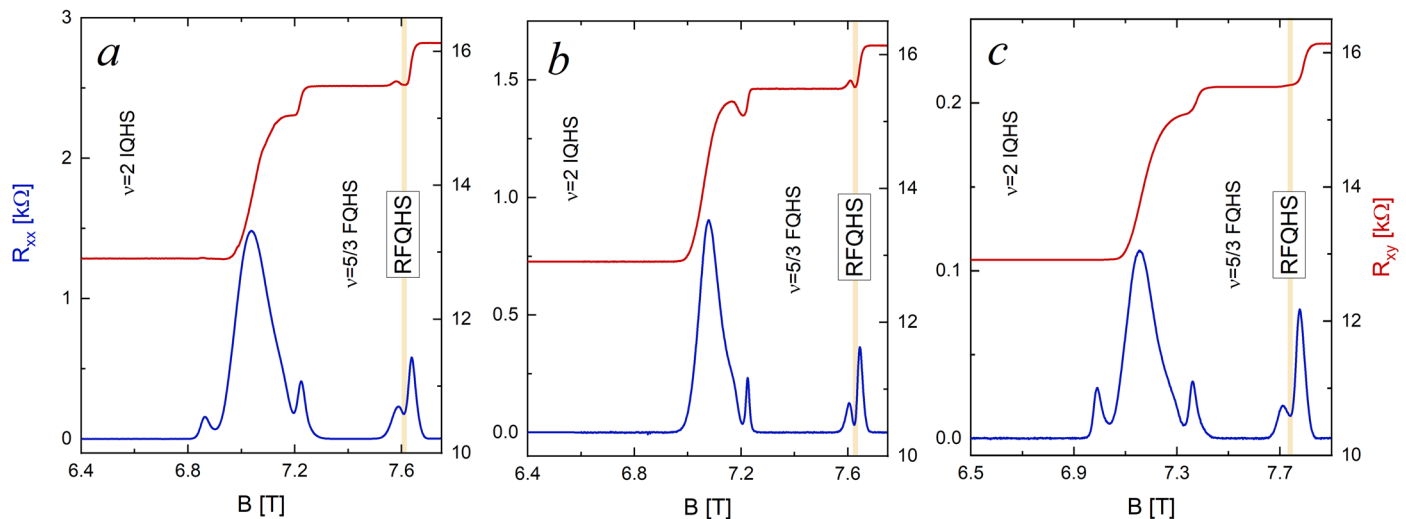
Extended data is available for this paper at <https://doi.org/10.1038/s41567-023-01939-2>.

Supplementary information The online version contains supplementary material available at <https://doi.org/10.1038/s41567-023-01939-2>.

Correspondence and requests for materials should be addressed to Gábor A. Csáthy.

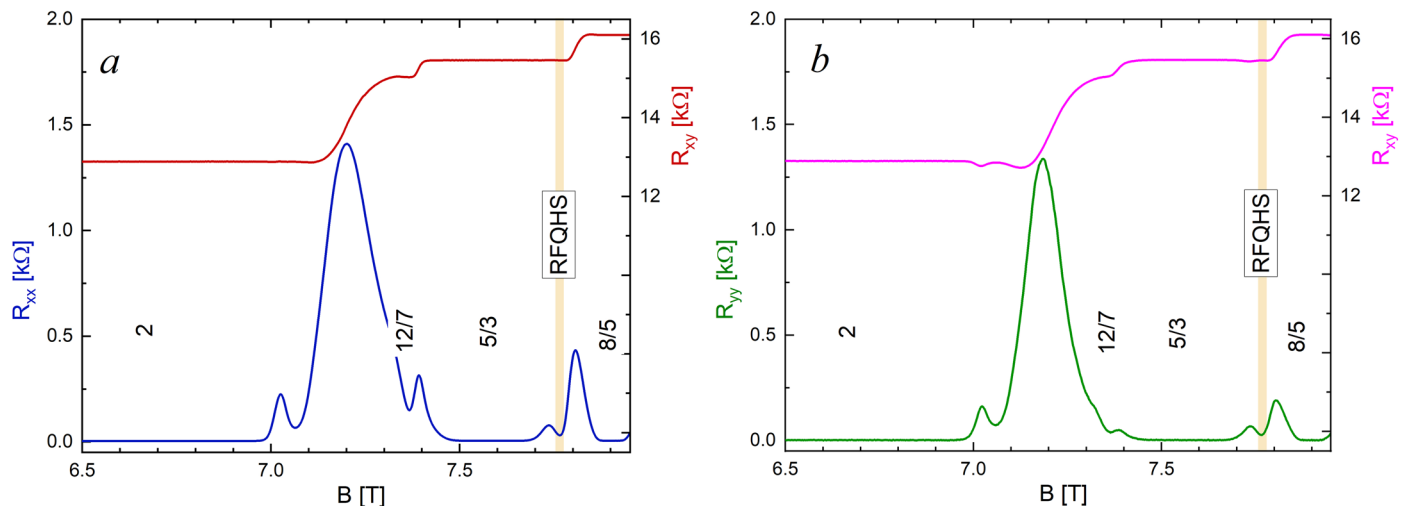
Peer review information *Nature Physics* thanks the anonymous reviewers for their contribution to the peer review of this work.

Reprints and permissions information is available at www.nature.com/reprints.



Extended Data Fig. 1 | Multiple observations of the RFQHS. Several longitudinal magnetoresistance R_{xx} and Hall resistance R_{xy} measurements. Panels **a** and **b** have data from Sample 1, collected after cycling the sample to

room temperature. Panel **c** has data from Sample 2. All panels exhibit the RFQHS, as evident from a splitting of the longitudinal magnetoresistance into two peaks and reentrance of the Hall resistance to $R_{xy} = 3h/5e^2$.



Extended Data Fig. 2 | The longitudinal magnetoresistance R_{xx} and R_{yy} as measured along two mutually perpendicular crystal directions and the Hall resistance. Data were collected from Sample 1 at $T = 12$ mK. While there are small but noticeable differences in the two longitudinal magnetoresistance traces,

at the formation of the RFQHS the longitudinal magnetoresistance is nearly vanishing for both crystal directions and it is nearly isotropic. Panels **a** and **b** show data collected along two mutually perpendicular crystal axes of the GaAs crystal.